ACS OMEGA

Open Access

This article is licensed under CC-BY-NC-ND 4.0

http://pubs.acs.org/journal/acsodf

Article

Evaluation of the Role of $[\{Cu(PMDETA)\}_2(O_2^{2-})]^{2+}$ in Open-Air Photo ATRP of Methyl Methacrylate

Arumugam Ramu and Kannapiran Rajendrakumar*

Cite This: *ACS Omega* 2024, 9, 44916−44930

Read Online

ACCESS | Metrics & More | Article Recommendations | Supporting Information

ABSTRACT: Herein, we report an open-air, photo accelerated atom transfer radical polymerization (ATRP) of methyl methacrylate (MMA) without employing any deoxygenating agent. Under open-air photo ATRP conditions, oxygen reversibly binds with $[\{Cu(PMDETA)\}_2(O_2^{2-})]^{2+}$(**1**) to form the required activator, which was demonstrated by simple benchtop oxygen/nitrogen purging experiments. The binding mode of oxygen in (**1**) ($\mu(\eta^2\text{-}\eta^2)$ peroxo dicopper(II)) was investigated using UV Visible-NIR, FT-Raman and X-ray photoelectron (XPS) spectroscopic techniques. DFT studies and electrochemical measurements further support the catalytic role of (**1**) in open-air photo ATRP. With the synergistic involvement of Cu(II)Br_2, PMDETA ligand and the intensity of light (365 nm, 4.2 mW cm^{-2}), a well-controlled rapid polymerization of MMA under open-air condition was achieved ($1.25 < Đ < 1.47$, 94% conversion in 200 min). The bromo chain end fidelity was exemplified by chain extension experiment, block copolymerization and MALDI-ToF analysis. Other monomers such as methyl acrylate, glycidyl methacrylate, and benzyl methacrylate were also polymerized under open-air condition with reasonable control over molecular weight and $Đ$. An open-air photo polymerization methodology would be fruitful for applications like photocurable printing, dental, optoelectronics, stereolithography, and protective coatings where simple but rapid photopolymerizations are desirable.

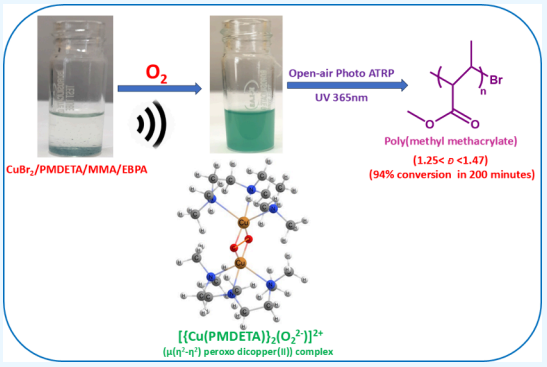

INTRODUCTION

In the last two decades, reversible deactivation radical polymerization (RDRP) methods such as atom transfer radical polymerization (ATRP)[1] and reversible addition−fragmentation chain transfer polymerization (RAFT)[2] have revolutionized the synthetic polymer field. IUPAC reported that the RDRP technique is one of the top ten emerging technologies that can change the world.[3] Among RDRP techniques, the ATRP continue to lead to advanced materials with applications in energy, microelectronics, biotechnology and defense.[4−6] With such a powerful tool, precisely designed polymers with complex molecular architectures and advanced functionality including block, star, and graft can be produced.[7] In ATRP, the activation−deactivation equilibrium can be controlled by external stimuli such as light, mechano (ultrasound) and electrochemical methods.[8] Particularly, the development of photo mediated controlled radical polymerization[9,10] opens a new sustainable alternative way to thermal initiated polymerizations of attractive features including mild reaction conditions, simple experimental setup, oxygen tolerance, low catalyst loading and spatiotemporal control. To attain control over polymerization, traditional ATRP methods need a high transition metal loading (up to 10000 ppm) under inert condition. In copper-based photo ATRP, the in situ (re)-generation of activator catalyst species by photo reduction of the deactivator drastically reduces the catalyst loading to below ∼100 ppm levels while providing oxygen tolerance.[11] The reduction process can be done in the presence of suitable additional photo initiator or photosensitizer including unimolecular radical initiators,[12] bimolecular radical initiators,[13] dyes,[14] semiconducting nanoparticles,[15,16] and metal carbonyl compounds[17] (indirect method), or the photo reduction (direct method) can be done in the absence of additional reagents. Other than copper, various transition metals including Fe,[11] Ir[18] and Ru[19] were also employed as effective photo catalysts in photo ATRP. In 2012, Hawker and co-workers exploited the power of photoredox catalyst, *fac*-$[Ir(ppy)_3]$ (ppy = 2-pyridylphenyl), for the photochemical initiation and control of the ATRP of MMA. Subsequently, metal-free photo ATRP of MMA using an organic based photoredox catalyst has also been reported.[20] Since then, several synthetic photoredox catalysts including phenothiazines, phenazines, phenoxazines, carbazoles, thienothiophenes, and oxygen-doped anthanthrene with favorable redox potential

Received: March 22, 2024
Revised: September 20, 2024
Accepted: October 1, 2024
Published: October 31, 2024

© 2024 The Authors. Published by American Chemical Society

Table 1. Summary of Key Works of Copper Based Oxygen Tolerant Photo ATRP of MMA[a]

Entry	Medium	Closed/Open	Time (h)	Conversion (%)	Đ	I_{eff}[b] (%)	Reference
1	DMSO	Closed	5	79	1.10	78	44
2	DMF	Closed	20	86	1.12	83	45
3	DMSO	Closed	5	83	1.19	80	46
4	Anisole	Closed	28	93	1.38	95.5	11
5	DMSO	Closed	6	65	1.10	80	47
6	Bulk	Open	3.3	94	1.47	89	This work

[a]All the polymerizations were performed without prior degassing. [b]I_{eff} − Initiator efficiency = Mol.wt (theo)/Mol.wt (expt).

have been demonstrated.[21] However, the extensive procedures for the synthesis of organo photoredox catalysts are seen as a blockade in the development of simple procedures. It made researchers to attempt naturally occurring riboflavin (vitamin B2),[22] curcumin[23] and commercially available, eosin Y,[24] erythrosine B[25] and fluorescein[26] for metal free photo ATRP systems. Recently, exploiting the benefit of visible light photo polymerization, acrylamides and methacrylates were polymerized under catalyst free conditions.[27]

Since oxygen can oxidize the transition metal catalyst and also indulge in radical scavenging,[28−30] prior deoxygenation of polymerizing mixture is much required. Freeze−pump−thaw cycles or sparging of inert gas or use of a glovebox[31−33] are the most common techniques employed to create an oxygen free environment. These laborious physical methods of degassing need sophisticated instruments, and monitoring systems limit the facile synthesis of polymeric materials with controlled molecular weight. To perform RDRP devoid of prior degassing, several "*oxygen tolerant*" methods have been developed.[34,35] In ATRP oxygen tolerance has been demonstrated using reducing agents such as zerovalent metals,[36] ascorbic acid,[37] tin(II) 2-ethylhexanoate[38] or phenols[39] via activator regeneration electron transfer (ARGET ATRP). As an alternate strategy, in the absence of external agent and stimulator, well controlled polymerization was also demonstrated by carefully adjusting the headspace of the reaction vessel.[40] Recently, fully oxygen tolerant well controlled polymerization of *N*-isopropylacrylamide (NIPAM) under open-air conditions has also been reported.[41] In another study, glucose oxidase (GOx) with sacrificial substrates such as glucose and sodium pyruvate has been used to continuously convert oxygen into carbon dioxide.[42] Similarly, in "*oxygen fueled*" open vessel aqueous ATRP, radicals were generated by oxygen in combination with GOx, horseradish peroxidase and copper complexes.[43] Seminal contributions from research groups of Mosnáek, Poly, and Matyjaszewski in oxygen tolerant photo ATRP of MMA under closed vessel conditions are listed in Table 1.

In previously reported works, well-controlled polymerizations were observed only under closed conditions. The residual oxygen present in the ATRP mixture was apparently self-deoxygenated by the combination of the ATRP mixture under irradiation. The time taken for self-deoxygenation is termed the induction period. After the induction period, polymerization proceeds as in the case of a conventional inert condition. The induction period can be reduced by adjusting the concentration of the ligand and the intensity of the irradiation. Recently, Matyjaszewski and his co-workers have demonstrated a fully open-air PICAR ATRP (photoinduced initiators for continuous activator regeneration) of N-isopropylacrylamide (NIPAM) or methyl acrylate (MA). The simultaneous regeneration of active form of copper catalyst and effective removal of oxygen has been observed in the presence of sodium pyruvate.[48] More recently, using the benefit of photo irradiation, several oxygen tolerant polymerizations have been demonstrated under ATRP condition.[49−51] On the other hand, Boyer's group developed the photoinduced electron/energy transfer RAFT (PET-RAFT) polymerization. Particularly, using the photocatalyst (PC) they demonstrated PET-RAFT polymerization in the presence of air.[52] In the subsequent work, in the presence of ascorbic acid, flavin mononucleotide (FMN) was used as a photo catalyst to mediate PET-RAFT polymerization under open-to-air condition.[53]

In order to elucidate the mechanism of oxygen tolerant photo ATRP, Haddleton et al. have investigated the individual and combined effect of ATRP components on the degree of self-deoxygenation using an oxygen probe device.[54] The exploration of the chemical coordination as well as structure activity relationship between oxygen and ATRP catalyst would provide better understanding about oxygen tolerant photo ATRP. Natural biological systems such as copper proteins, hemocyanin and tyrosinase utilize the reversible binding of O_2 at the copper site for oxygen transport. Like these biological systems, several synthetically derived "*copper-dioxygen*" assemblies exhibit excellent reversible oxygen uptake under mild conditions. For instance, the copper-dioxygen complex of tris(2-pyridylmethyl)amine (TPMA) or Me_6Tren exhibits reversible oxygen binding at copper center by forming equilibrium mixture of "*side-on*", "*end-on*" superoxide and peroxide level species[55] (Scheme 1).

Scheme 1. Copper-Dioxygen Isomeric Complexes

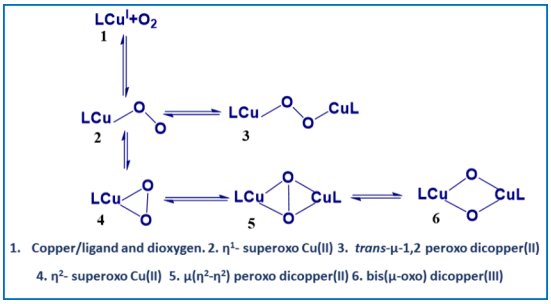

Notably, Karlin and co-workers demonstrated the clean reversible oxygen binding ability of [{Cu-(PMDETA)}$_2$(O_2^{2-})]$^{2+}$ through "*warm/cooling*" benchtop experiments.[56] More recently, Anastasaki and co-workers have reported the reversible binding of oxygen at copper center through ARGET ATRP mechanism.[57] In that case, the formation of a *superoxido* [Cu(I)(Me_6Tren) O_2] complex was proven to be responsible for the reversible oxygen uptake at room temperature. Utilizing the same catalytic system, they

https://doi.org/10.1021/acsomega.4c02773
ACS Omega 2024, 9, 44916−44930

have demonstrated well controlled polymerization of both hydrophilic and hydrophobic monomers under mild conditions. However, in the absence of light, polymerization of methyl acrylate requires more than 8 h to reach high monomer conversions. Upon UV irradiation, a significant enhancement over the polymerization rate was observed (conversion >90% within 2 h; $Đ = 1.07$). An enhanced rate of polymerization was attributed to the faster regeneration of active catalyst (Cu(I)Br) from superoxido copper complex under UV irradiation.[58] More notably, the induction period was eliminated, which is in stark contrast with conventional photo-ATRP systems. Schindler and co-workers have investigated the unusual stability of $[Cu^{II}(Me_6Tren)(O_2^{\bullet-})]^+$ under ambient conditions.[59]

Inspired by these previous works, herein, we present a simple polymerization procedure to synthesize well controlled PMMA under open-air conditions whereby oxygen tolerance was achieved by the regeneration of the active form of catalyst and formation of $[\{Cu\ (PMDETA)\}_2(O_2^{2-})]^{2+}$ (**1**) without employing external additives. In terms of green chemistry perspective of presented methodology, two important principles were considered. Accordingly, achieving high monomer conversion in bulk polymerization ("*prevent waste*", *Principle 1) and* oxygen tolerant polymerizations ("*less hazardous synthesis*", *Principle 3*) were addressed. We believe that this methodology would circumvent the laborious and time-consuming deoxygenation steps while providing access to the facile synthesis of PMMA in a quick time.

EXPERIMENTAL SECTION

Methyl methacrylate, methyl acrylate, glycidyl methacrylate and benzyl methacrylate was received from Aldrich chemicals. The inhibitor was removed by being passed through a basic alumina column prior to use. Ethyl α-bromo phenylacetate, (EBPA; Alfa-Asar,97%), ethyl α-bromoisobutyrate (EBiB; Sigma-Aldrich, 98%) *N,N,N′,N″,N‴*-pentamethyldiethylenetriamine (PMDETA; Sigma-Aldrich, 99%), Copper(II) bromide-($CuBr_2$;Sigma-Aldrich,99%), tris[2-(dimethylamino)ethyl]-amine (Me_6Tren; TCI-India, 99%). Solvents from Avra chemicals were used as received. ^{1}H NMR spectra were recorded on a Bruker 400 MHz instrument. Spectra were reported relative to Me_4Si (δ 0.0 ppm) or DMSO-d6 residual peak (2.56 ppm). All monomer conversions were calculated using ^{1}H NMR studies. Molecular weight and dispersities ($Đ$) of polymers were determined by using Gel Permeation chromatography (GPC). The GPC system was equipped with a JASCO PU-4180 RHPLC pump and JASCO RI-4030 refractive index detector using WATERS Styragel HR4E-(DMF) 4.6 × 300 mm column with DMF as an eluent at a flow rate of 0.5 mL/min at 50 °C. The apparent molecular weights (Mn) and dispersities $Đ$, were determined using linear poly(methyl methacrylate) (Mn = 2000−100000) standards using ChromNAV Ver.2 software. UV Visible NIR spectrum were recorded in Agilent Cary 5000, Wavelength range: 175−3300 nm, double out-of-plane Littrow Monochromator, Tungsten-halogen and deuterium; R 928 Photomultiplier detector. FT- Raman measurements were taken by BRUKER RFS 27 Multi RAM FT Raman Spectrometer with a scan range 4000−50 cm^{-1} equipped with a purgeable sealed optics housing. The source is Nd:YAG laser (1064 nm); in addition, there is a white light source for Raman background correction and built in alignment lamp for sample alignment and calibration. The sample stage is pre aligned with computer-controlled z-positioning. Scattered light is collected at 180° using a high throughput lens. XPS studies were probed using XPS microprobe (Shimadzu Aixs Supra XPS, kratos analytical). 1.6 eV step size was employed for wide scan spectra. The individual core level Cu 2p, O 1s, and C 1s spectra were obtained with a step size of 0.05 eV. DFT calculations were performed using the GAUSSIAN 09 program package with the aid of the GaussView visualization program. The ground state geometries were fully optimized using the hybrid B3LYP functional methods in combination with the 6-31G (d,p) basis set for lighter elements (C, H, and O) and the LanL2DZ effective core potential for metals (Cu and Br). All geometries were optimized to zero negative vibrational frequency to ensure global minima. The fractional contributions of various groups to each molecular orbital were calculated by using Gausssum, and Chemissian was used for spectrum analysis. The excited state properties of the optimized ground state geometry were calculated with the 25 roots using the time-dependent density functional (TD-DFT) formalism using the same level of theory. MALDI-ToF-MS was measured by using a Bruker MALDI-TOF (UltrafleXtreme II) mass spectrometer. solutions in THF of DCTB (trans-2-[3-(4-*tert*-Butylphenyl)-2-methyl-2-propenylidene] malononitrile) as the matrix (30 mg mL^{-1}), sodium trifluoroacetate as the cationisation agent (1.0 mg mL^{-1}) and PMMA-Br (1 mg mL^{-1}) were prepared. 40 μL of matrix solution was mixed with 5 μL of cationization agent solution and 10 μL of sample solution, and 1 μL of the mixture was drop casted on the target plate and dried under room temperature and the spectrum was recorded.Cyclovoltammetry measurements were done using Metrohm Autolab potentiostat controlled by nova 2.1.6 software. A three-electrode system that comprises a glassy carbon electrode (0.07 cm^2 dia), a Pt wire, and Ag/AgCl (3 M KCl) as working, counter, and reference electrodes, respectively, were used. The electrolyte solution is a combination of s 0.01 M $CuBr_2$/PMDETA in acetonitrile and Bu_4 NBF_4 with a scan rate of 0.5 V s^{-1}).

General Polymerization Procedure (under inert atmospheric condition). $CuBr_2$ (4.2 mg, 0.1 equiv) was added to 7 mL of a clean glass vial. Then the vial was tightly sealed and subjected to five alternate vacuum and nitrogen cycles. Then PMDETA (4 μL, 0.1eq), degassed MMA (4 mL, 200eq) and EBPA (32.8 μL,1.0eq) were added under nitrogen atmosphere. This solution was irradiated under two 8 W UV (365 nm) lights (4.2 mW cm^{-2}). Samples were taken at subsequent intervals for GPC analysis and monomer conversion calculations.

General Polymerization Procedure (under non degassed and closed condition). In a 7 mL glass vial, $CuBr_2$ (4.2 mg, 0.1 equiv), PMDETA (4 μL, 0.1 equiv), nondegassed MMA (4 mL, 200 equiv), and EBPA (32.8 μL, 1.0 equiv) were added under open atmosphere. Then the vial was sonicated for 5 min and capped. This solution was irradiated under two 8W UV lights (365 nm, 4.2 mW cm^{-2}). Samples were taken at subsequent intervals for GPC analysis and monomer conversion calculations.

General Polymerization Procedure (under completely open atmosphere). In a 7 mL glass vial, $CuBr_2$ (4.2 mg, 0.1 equiv), PMDETA (4 μL, 0.1 equiv), nondegassed MMA (4 mL, 200 equiv), and EBPA (32.8 μL,1.0 equiv) were added under open atmosphere. Then the vial was sonicated for 5 min. Without capping the vial, the solution was irradiated under fully open atmosphere with two 8W UV lights (365 nm,

https://doi.org/10.1021/acsomega.4c02773
ACS Omega 2024, 9, 44916−44930

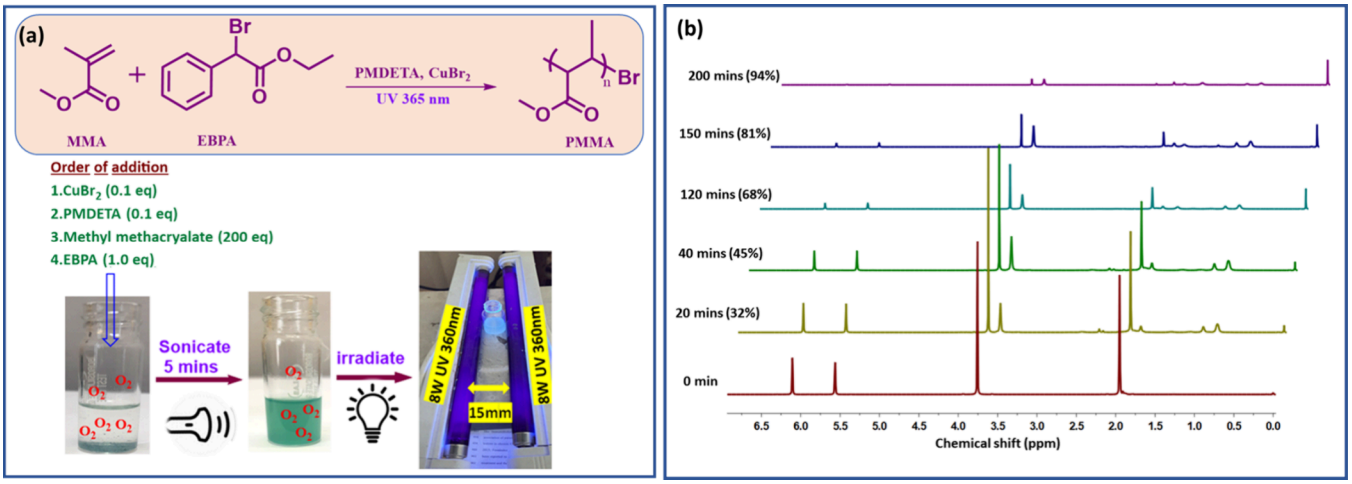

Figure 1. Open-air photo ATRP of MMA. (a) Methodology employed. (b) ^{1}H NMR spectra of samples taken at subsequent intervals.

Table 2. Optimization Studies on Open-Air Photo ATRP of MMA[a]

Entry	[MMA]/[$CuBr_2$]/[PMDETA]/[EBPA]	Time(min)	α (%)	Mn_{theo}	Mn_{GPC}	$Đ$	I_{eff} (%)
1	200/0.1/0.1/1	200	94	18800	20100	1.47	89.63
2	200/0.1/0.1/1	200	95	19000	20000	1.38	95.00
3	200/0.1/0.1/1	200	80	16000	16100	1.29	99.40
4	200/0/0.1/1	200	25	5000	92000	1.53	5.43
5	200/0.1/0/1	200	66	13200	36800	1.49	35.87
6	200/0.1/0.1/0	120	-	-	-	-	
7	200/0.1/0.1/1	2160	65	13000	25000	1.39	52.00
8	200/0.1/0.1/1	200	83	16600	22000	1.62	75.45

[a]Bulk polymerizations of MMA were performed in 7 mL unsealed vial using domestic two 8W UV lamp (365 nm, 4.2 mW cm^{-2}) under ambient atmosphere. Entry 2 nondegassed closed vial. Entry 3 inert condition. Entry 7 - dark condition Entry 8 - without prior sonication. Conversions(α) were calculated by ^{1}H NMR. Experimental molecular weight and dispersity $Đ$ were determined by GPC analysis.

4.2 mW cm^{-2}). Samples were taken at subsequent intervals for GPC analysis and monomer conversion calculations.

General Chain Extension Experiments (under completely open atmosphere). In a 7 mL glass vial, $CuBr_2$ (4.2 mg, 0.1 equiv), PMDETA (4 μL, 0.1 equiv), nondegassed MMA (4 mL, 100 equiv), and EBPA (65.6 μ 1.0 equiv) were added under open atmosphere. Then the vial was sonicated for 5 min. Without capping the vial, the solution was irradiated under fully open atmosphere with two 8W UV lights (365 nm, 4.2 mW cm^{-2}4.2 mW cm^{-2}). PMMA-Br with Mn 4700 and $Đ$ = 1.29. The chain extension polymerization was performed by using the macroinitiator. The chain extended polymer was shown to have Mn = 19200 and $Đ$ = 1.52. Similarly, block copolymerization was also performed using benzyl methacrylate as a second monomer.

General Polymerization Procedure for Styrene, Methyl Acrylate, Benzyl Methacrylate and Glycidyl Methacrylate (under completely open atmosphere). For styrene alone, the target degree of polymerization was 50 and for all the other monomers it was set for 200. In a typical procedure, $CuBr_2$/PMDETA/Monomer/EBiB were taken in a 7 mL open glass vial, with a mole ratio of 0.1:0.1:200:1.0 respectively followed by sonication for about 5 min. Without capping the vial, the solution was irradiated under fully open atmosphere with two 8W UV lights (365 nm, 4.2 mW cm^{-2}). Samples were taken at subsequent intervals for GPC analysis. Conversions were calculated by ^{1}H NMR.

RESULTS AND DISCUSSION

Extending the scope of transition metal catalyzed controlled radical polymerization to all types of vinyl monomers itself remains a challenge, especially for the hydrophilic monomers with carboxylic acid, amine, and hydroxyl functionalities due to the complex formation and solvent interaction with the metal catalyst. As a result, even under inert conditions, there is no universally adaptable procedure that encompasses all type of monomers. Polymerizations under limited oxygen levels/closed systems were limited only for a few of the hydrophilic monomers having a high kp. Application of fully oxygen tolerant controlled polymerization strategies for the low kp monomers like MMA is less documented. Keeping this in mind, we have aimed at the development of fully oxygen tolerant and additive free, photo ATRP of MMA. Initially, a trial set of polymerizations of MMA was performed with $CuBr_2$/PMDETA catalytic system in the presence of EBPA initiator with the domestic UV lamp activation.

As depicted in Figure 1a, $CuBr_2$, PMDETA, MMA and EBPA were sequentially placed in a 7 mL vial. Without any degassing, the unsealed vial was sonicated for 5 min and irradiated with the domestic 8W UV lamp (365 nm, 4.2 mW cm^{-2}). ^{1}H NMR analysis (Figure 1b) revealed that the polymerization of MMA under open-air photo ATRP condition was faster, as 94% conversion was reached in 200 min. Also, from GPC analysis, it was found to be a close correlation between the experimental and theoretical molecular weight with reasonable dispersity (entry 1, Table 2). The rate of polymerization was considerably faster when compared to

https://doi.org/10.1021/acsomega.4c02773
ACS Omega 2024, 9, 44916−44930

previously reported oxygen tolerant polymerizations of MMA.[44−47] More interestingly, we did not observe any significant induction period.

To understand the role of oxygen in photo ATRP of MMA, polymerizations were performed under two different conditions. Under nondegassed closed condition, improved control over molecular weight and dispersity compared to open-air condition was observed (entry 1, Table 2). It should be noted that the better control under nondegassed closed condition could be attributed to the absence of continuous oxygen diffusion into the reaction vessel. It should also be noted that the control over molecular weight and dispersity was even better in the case of the inert condition (entry 1, Table 3). These results suggest that the rate of oxygen diffusion into the reaction vessel substantially influence the control over molecular weight and dispersity. Control experiments were carried out in the absence of either one component such as $CuBr_2$, EBPA, PMEDTA and light. Accordingly, in the absence of $CuBr_2$ or ligand (PMDETA), uncontrolled polymerizations were observed (entries 4 and 5, Table 2). No polymerization was observed in the absence of initiator (EBPA) (entry 6, Table 2) and very slow polymerization was observed in the dark (entry 7, Table 2). These results indicate their mandatory role to exhibit controlled radical polymerization under open-air condition. Previous works on oxygen tolerant photo ATRP of MMA rely on regeneration of activator (CuBr(I)/L) by photo reduction of deactivator ($CuBr_2$(II)/L). In these cases, under a closed vessel condition, controlled polymerization starts only when all the residual oxygen was consumed by polymerizing mixture.[44−47] More notably, due to the continuous oxygen diffusion, no polymerization was realized under completely open-air condition. Indeed, in these works, the lack of polymerization under dark condition even after 32 h also supports the previously proposed mechanisms. Nonetheless, in the current study, we were able to realize an unprecedented rapid controlled polymerization under open-air photo irradiation condition. In contrast to the previous reports, we also observed very slow polymerization (~83% conversion in 2160 min) even under open-air dark condition (entry 8, Table 2). It should be noted that the polymerization of MMA in the presence acetonitrile (33% V/V) under open-air condition yielded only 12% conversion in 14 h. This sluggish rate of polymerization could be attributed to the significant evaporation of the reaction mixture during open-air polymerization, whereas a reasonable rate of polymerization was observed when reaction was performed under closed vessel condition. As shown in the Figure S1a, a very low induction period was observed. The molecular weight increased linearly as a function of monomer conversion (Figure S1b). GPC traces of kinetic samples are given in Figure S1c.

Table 3. Redox Potentials of [$CuBr_2$/PMDETA] Measured by Cyclic Voltammetry in Acetonitrile at Room Temperature

Entry	[$CuBr_2$/PMDETA]	[a] $Ea_{p,a}$(V)	[a] $E_{p,c}$(V)	[b] $E_{1/2}$(V)	[c] ΔE (mV)	[d] i_b/i_f
1	0.01 M nitrogen saturated	0.211	−0.100	0.056	111	1.07
2	0.01 M oxygen saturated	0.132	−0.178	−0.046	310	0.83

[a] $E_{p,a}$ and $E_{p,c}$ are the peak potentials of the oxidation and reduction waves respectively. [b] $E_{1/2} = (E_{p,a} + E_{p,c})/2$; [c] $\Delta E = E_{p,a} - E_{p,c}$; [d] i_b/i_f is the ratio of backward to forward peak current

Kinetic Investigation of Photo ATRP of MMA under Open-Air, Nondegassed Closed and Inert Conditions. Detailed kinetic investigation of photo ATRP of MMA under open-air, nondegassed and inert conditions revealed that the polymerizations proceeded with linear first-order kinetic behaviors (Figure 2a). Moreover, the molecular weight increased linearly as a function of monomer conversion (Figure 2b). The GPC traces of kinetics are given in Figure S2 (a) open-air, (b) closed, and (c) inert condition.

Mechanistically, in the case of photo accelerated controlled polymerization under open-air conditions, the regeneration of the activator complex could be achieved through the photo reduction of deactivator $CuBr_2$/PMDETA. However, the incidence of polymerization even under dark open-air conditions implies the regeneration of activator in the absence

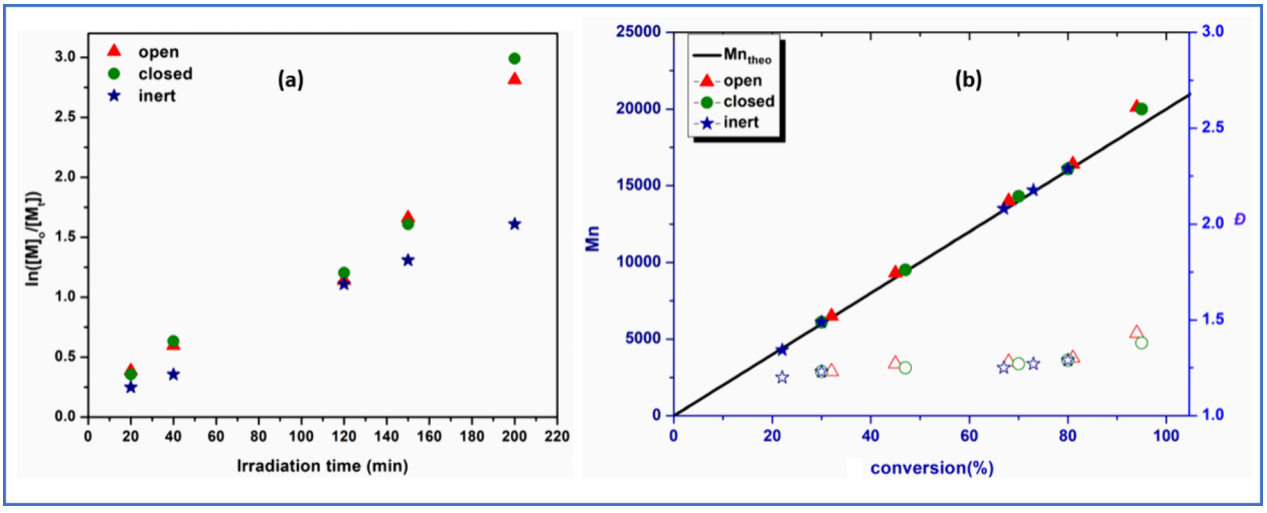

Figure 2. Photo ATRP of methyl methacrylate under open-air, closed and inert conditions. a) Kinetic plot b) Evolution of molecular weight (solid points) and dispersity Đ (hollow points). Experimental condition: MMA/EBPA/PMDETA/$CuBr_2$= 200/1/0.1/0.1., 8W domestic UV lamp. λ=365 nm, 4.2 mW cm^{-2}.

https://doi.org/10.1021/acsomega.4c02773
ACS Omega 2024, 9, 44916−44930

of light by different reaction pathway. Though the mechanism of the polymerization under dark condition was unclear, previous research[39] described that reversible oxygen binding of (**1**) could result in the formation of equilibrium mixture of copper-dioxygen complexes and ATRP activator complex. These results prompted us to investigate the mechanism in more detail.

Mechanistic Investigation. Majority of currently available experimental data suggests oxygenation of copper(I) complexes to form Cu (II) superoxo species which would then react with second equivalent of the copper(I) complex to form Cu (II) peroxo complex (Scheme 1).[60] However, the structure of ligands that differ by chelate ring sizes, donor atoms, or their overall formal charges dictates the binding mode of oxygen at the copper center. For example, under similar experimental condition, the oxygenation of Cu(I)/PMDETA complex yield the equilibrium mixture of Cu (II) superoxo and Cu (II) peroxo complexes, whereas the oxygenation of Cu(I)/Me_6Tren complex yield only *end-on* Cu (II) superoxo complex.[61] More importantly, the mode of binding of oxygen with the copper metal center decides the stability of oxygenated copper complexes. By considering all the previously reported mechanisms[60] for copper- dioxygen species and controlled nature of polymerization under open-air atmosphere from present work, we hypothesized the shuttling of one electron reversible oxygen binding cycle in (**1**), similar to the activation/deactivation cycle in ATRP mechanism, resulting in the formation of Cu(I) and Cu (II) species. Since the reversible oxygen binding ability of (**1**) has already been demonstrated at low temperature,[39] we strived to exemplify the similar kind of reversible oxygen binding of $CuBr_2$/PMDETA complex under ambient ATRP condition. Accordingly, in a benchtop experiment, the ATRP mixture (MMA/EBPA/PMDETA/$CuBr_2$= 200/1/0.1/0.1equiv) was prepared under both inert and open-air conditions. The mixture thus prepared remained colorless and did not show any characteristic color change under nitrogen (inert) atmosphere even after 15 min of sonication (Figure 3). The same mixture when purged with oxygen for 30 min, the colorless solution turns into green color, suggesting that the oxygenation of $CuBr_2$/PMDETA complex was successful. Meanwhile, the same ATRP mixture prepared under open-air atmosphere showed an intense green after sonication for a period of 5 min, which was presumably attributed to the formation of (**1**). Parallelly, 30 min purging of nitrogen gas into green color ATRP mixture under open atmosphere, the initially formed green color almost disappeared. These observations could be correlated to reversible oxygen binding at copper center under ambient condition.

To verify the identity of oxygenated species in the ATRP mixture, the aforementioned ATRP solutions were subjected to UV Visible-NIR analysis. As shown in the Figure 4, the absorption at 690 nm (red line) of the ATRP mixture prepared under ambient atmosphere is attributed to the characteristic absorption of (**1**). In the case of inert atmosphere, we did not observe any characteristic spectral feature at 690 nm (pink line), which precludes the existence of (**1**). It is important to mention that the increase in absorption at 690 nm of the ATRP solution after 90 min (black line) irradiation indicates the favorable formation of (**1**) during the polymerization. These results match well with the literature on this oxygen coordinated complexes.[56]

As per previous reports,[56,61] the oxygenation of ATRP components would likely to yield the required equilibrium

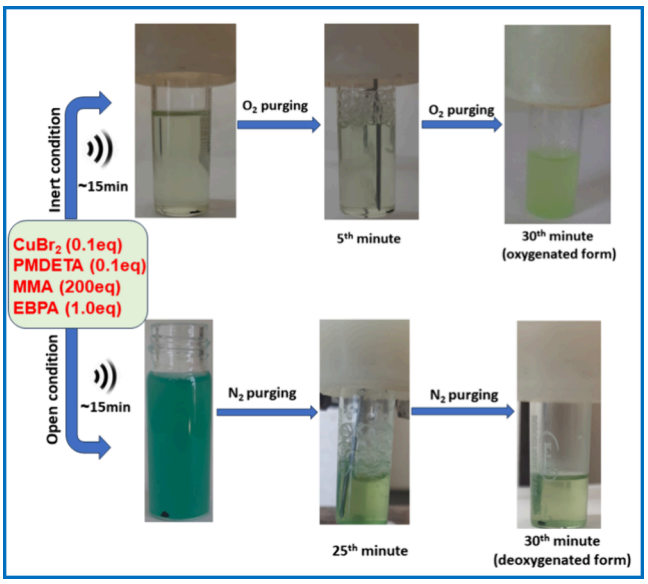

Figure 3. Bench top experiments demonstrating the reversibility of oxygen with copper-PMDETA complexes in ATRP mixture (MMA/EBPA/PMDETA/$CuBr_2$ = 200/1/0.1/0.1eq; taken in a glass vial 7 mL tightly closed with a septa).

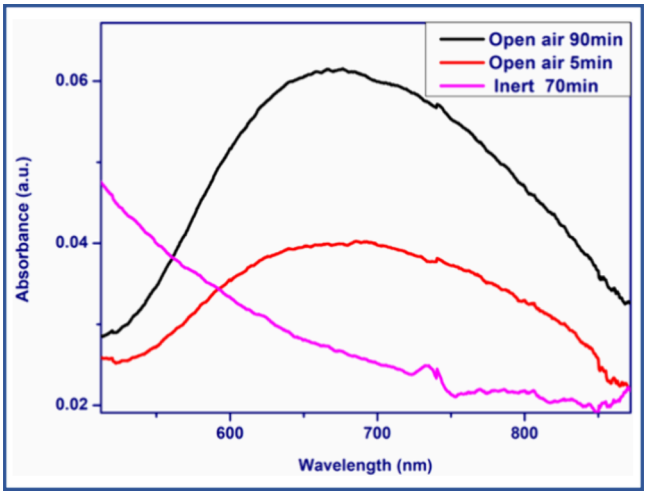

Figure 4. UV Visible NIR spectra of polymerization samples in open and inert conditions with the following system: MMA/EBPA/PMDETA/$CuBr_2$ = 200/1/0.1/0.1; domestic 8W UV lamp; λ =365 nm; 4.2 mW cm^{-2}.

mixture of Cu(I) and Cu (II) complex during the polymerization. XPS studies were done to determine the oxidation state of copper species during open-air polymerization. Figure 5 shows the XPS survey spectrum of sonicated ATRP mixtures at 5 min (red line) and 90 min (black line). The two ATRP mixtures show similar characteristic signals of Cu 2p, 3s, 3p, 3d, O 1s and Auger lines. The corresponding high-resolution core level spectra of sonicated ATRP mixtures at 5 and 90 min were plotted after carbon correction using a binding energy of 284.8 eV for C 1s peak.

Comparing the core level spectral features of ATRP mixture after 5 min of sonication (Figure 6a) and 90 min of sonication (Figure 6b), it was possible to determine the oxidation state of copper catalyst during the polymerization. The main peak of Cu 3/2 for both the samples centered at 931.8 and 931.7 eV are due to the coexistence of Cu(I) and Cu (II)[62] during the

https://doi.org/10.1021/acsomega.4c02773
ACS Omega 2024, 9, 44916−44930

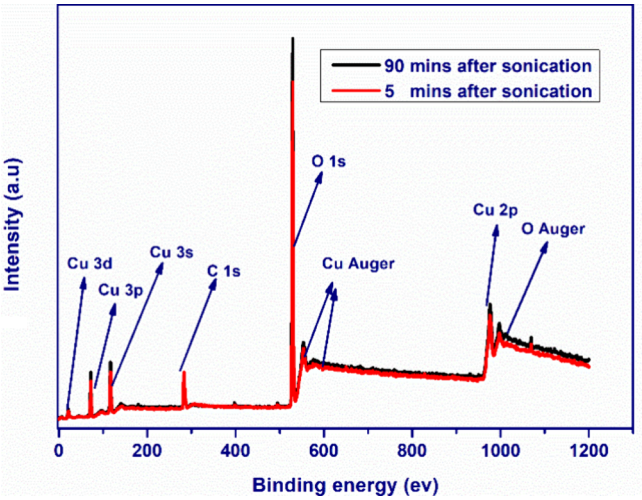

Figure 5. Survey XPS survey spectra of samples at 5 min(red)s and 90 min(black) after sonication and irradiation. Experimental condition: MMA/EBPA/PMDETA/$CuBr_2$ = 200/1/0.1/0.1; 8W domestic UV lamp, λ=365 nm; 4.2 mW cm^{-2}.

polymerization. Examining the core level spectra of the O 1s of ATRP mixture after 5 min of sonication (Figure 6c) and 90 min of sonication (Figure 6d), the peaks centered at 530.28 and 530.34 eV correspond to the oxygen species which presumably bound with copper catalyst. This assumption may be related to the formation of oxygenated copper catalyst. It should be noted that the shift observed in the binding energy of O 1s peak (0.6 eV) and increased peak area at different sonication time interval (5 and 90 min) indicates the intake of oxygen amount being increased[63] as the polymerization progress. Therefore, we conclude that the formation of the equilibrium mixture of oxygenated copper catalyst was responsible for the controlled polymerization of MMA under ambient atmosphere.

Since UV Visible NIR and X-ray photoelectron spectroscopy results reveal the existence of oxygenated copper catalyst in the ATRP mixture, we employed FT-Raman spectroscopy to determine the binding mode of oxygen on copper catalyst.

As can be seen from the Raman spectra of ATRP mixtures after 5 min of sonication (Figure 7a) and 90 min of sonication (Figure 7b), the stretching vibration at 830 cm^{-1} observed in both the samples corresponding to O−O stretch which could be correlated to the existence of (**1**). More evidently, the intense vibration at 600 cm^{-1} indicates peroxide bound in a side-on manner bridging the copper(II) ions. These vibrations and respective energies are consistent with the literature report.[64]

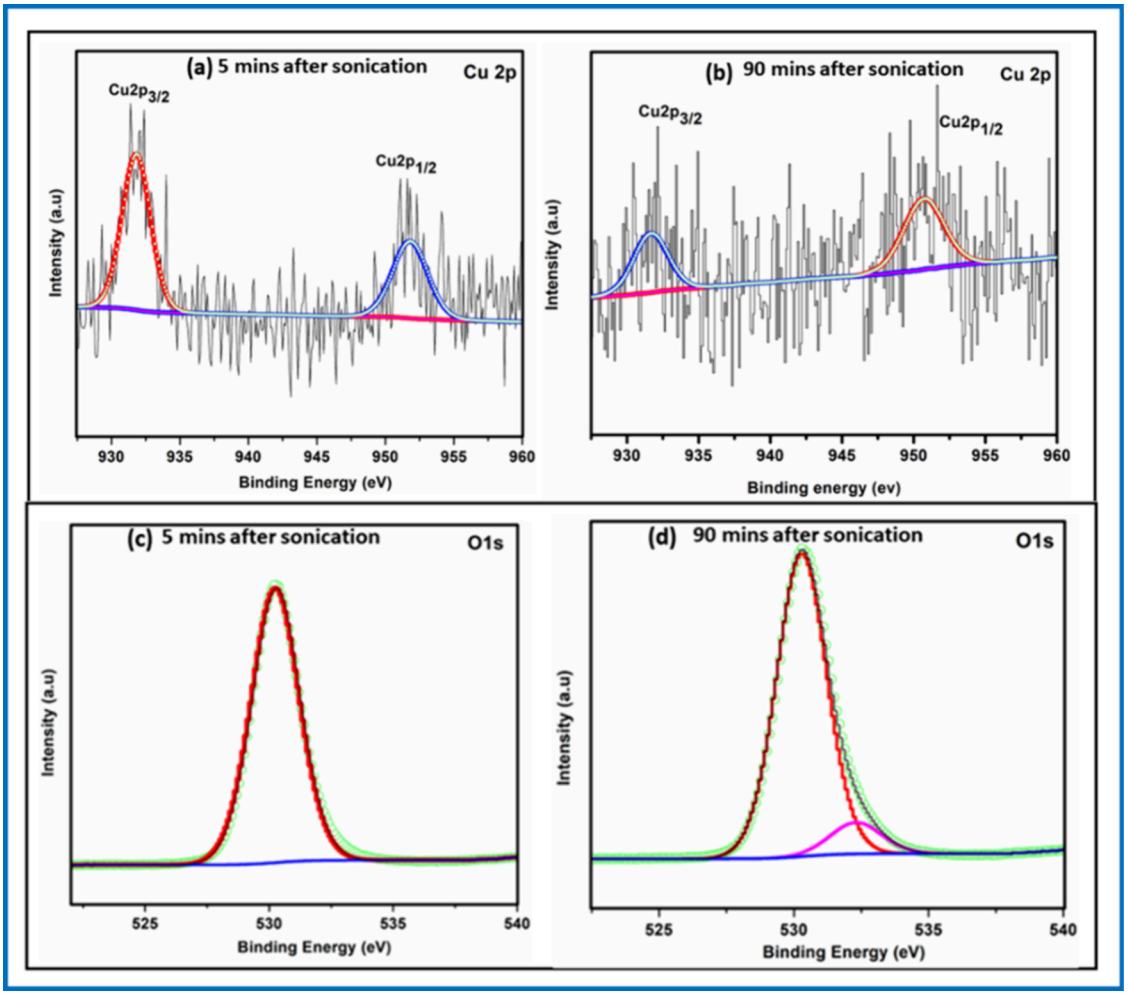

Figure 6. Core level spectrum of Cu 2p of the ATRP mixture after (a) 5 min of sonication and (b) 90 min of sonication. Core level spectrum of O 1s of the ATRP mixture after (c) 5 min of sonication and (d) 90 min of sonication.

https://doi.org/10.1021/acsomega.4c02773
ACS Omega 2024, 9, 44916−44930

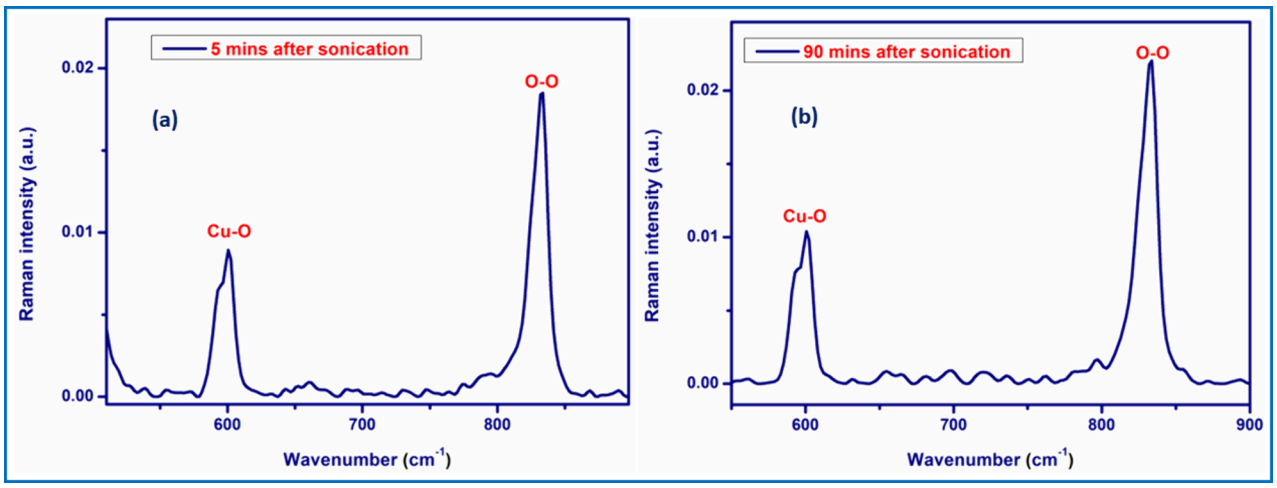

Figure 7. FT-Raman spectra of sonicated ATRP mixture after (a) 5 min of sonication and (b) 90 min of sonication. Experimental condition: MMA/EBPA/PMDETA/$CuBr_2$ = 200/1/0.1/0.1; 8W domestic UV lamp; λ = 365 nm; 4.2 mW cm^{-2}.

Electrochemical Characterization of (1). The redox properties of $CuBr_2$/PMDETA under nitrogen oxygen saturated condition were investigated by cyclic voltammetry (CV) as shown in Table 3.

As shown in Figure 8, the [$CuBr_2$/PMDETA] complex under nitrogen and oxygen saturated condition shows a reversible redox wave at $E_{1/2}$ = 56 and −46 mV vs Ag/AgCl, respectively.

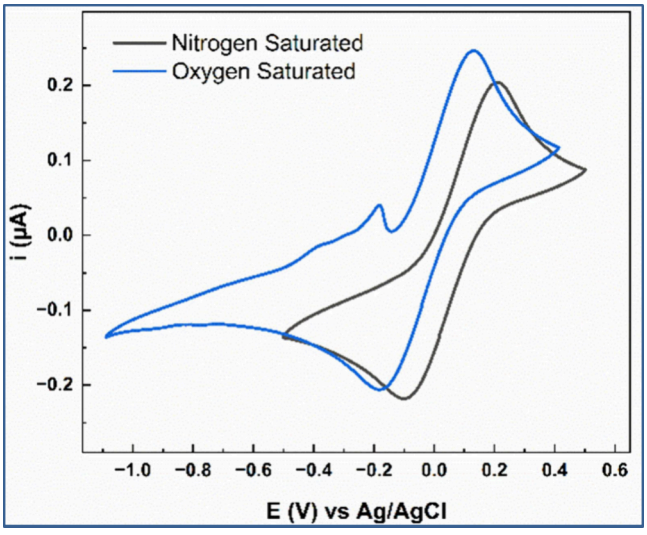

Figure 8. Cyclic voltammograms of oxygen saturated and nitrogen saturated $CuBr_2$/PMDETA complexes in acetonitrile (0.1 M Bu_4NBF_4; scan rate: 0.5 V s^{-1}). $[CuBr_2/PMDETA]_0$: 0.01 M.

These values suggested that oxygen saturated complex could be a more active ATRP catalyst than nitrogen saturated. Peak separation between the anodic and the cathodic peaks of both the catalytic species indicate good reversibility and quasi-reversible nature of the electron transfer.[65,66] Moreover, the coordination of oxygen with [$CuBr_2$/PMDETA] favors the stabilization of electrochemically generated (Cu(I)) activator species.

Computational Calculations. To get more insight into the structural features of oxygenated copper/PMDETA complex in ATRP solution, we performed DFT calculations. According to Scheme 1, at least five oxygenated copper/PMDETA species may be present in the ATRP solution as an equlibrium mixture. However, DFT calculations revealed only $\mu(\eta^2\text{-}\eta^2)$ peroxo dicopper(II), "*side-on*" η^2-suproxo Cu(II) and "*end-on*" η^2-superoxo Cu(II) complexes (Figure 9) were energetically favorable under our polymerization condition. Computationally calculated bond distances of Cu−O and O−O in $\mu(\eta^2\text{-}\eta^2)$ peroxo dicopper(II), side-on η^2-superoxo Cu(II), and end-on η^2-superoxo Cu(II) were consistent with the reported values.[56] It should be noted that among these three structures, the $\mu(\eta^2\text{-}\eta^2)$ peroxo dicopper(II) complex is more energetically accessible as evidenced by HOMO−LUMO calculations. For instance, the HOMO−LUMO energy gap for $\mu(\eta^2\text{-}\eta^2)$ peroxo dicopper(II) i.e., (**1**) was 1.95 eV (Figure 10), which is relatively larger than the other two structures.

Proposed Mechanism. In order to elucidate the mechanism of copper-based photo ATRP, Anastasaki and co-workers performed several control experiments by systematically varying individual components of the ATRP mixture.[67] In that proposed mechanism, the photo excited ligand (Me_6Tren) transfers the electron to the alkyl halide initiator leading to a homolytic cleavage of C−Br bond. In the subsequent insightful work, using pulsed-laser polymerization (PLP), and electro-spray-ionization mass spectrometry (ESI-MS), a more detailed mechanism, confirming the regeneration of active form of catalyst Cu(I)Br from initially added $CuBr_2$ using the photo excited amine ligand has been proposed.[68] A similar mechanism was reported by Poly[45] and co-workers, wherein the photo ATRP of MMA in the presence of residual oxygen using triethylamine and various amine-based ligands were demonstrated. On the other hand, Mosnáček[44] and Matyjaszewski[69] have proposed a slightly different mechanism in which the oxidation of Cu(I)Br/L by oxygen to form $CuBr_2(O_2)$/L which in turn undergo reduction in its excited state by gaining an electron preferably from ligand or other electron donor species in their respective excited states yielding CuBr/L and oxidized form of ligand. Recently, a mechanism involving reversible binding of oxygen with CuBr/(Me_6Tren) under ARGET and photo ATRP conditions were proposed. Based on the previously reported mechanisms, in the current study, the regeneration of activator(Cu(I)Br/PMDETA) possibly attributed to the combination of reversible oxygen binding of (**1**) and photo reduction of excited PMDETA

https://doi.org/10.1021/acsomega.4c02773
ACS Omega 2024, 9, 44916−44930

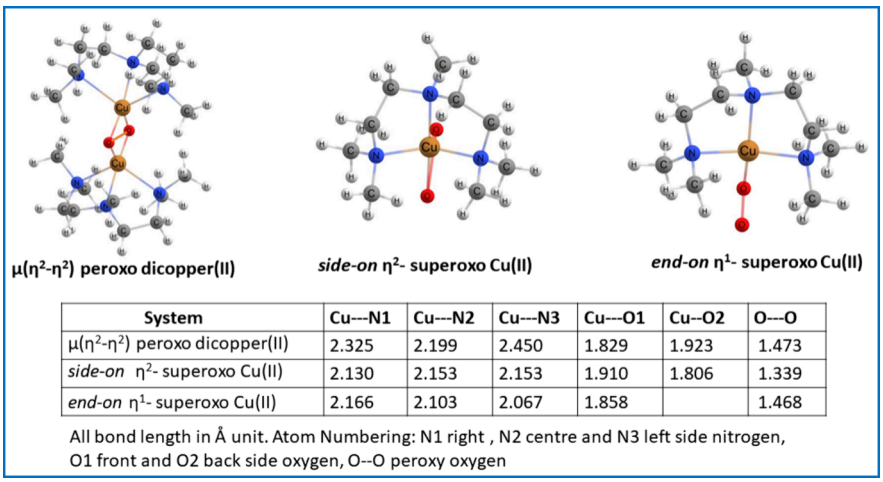

System	Cu---N1	Cu---N2	Cu---N3	Cu---O1	Cu--O2	O---O
μ(η²-η²) peroxo dicopper(II)	2.325	2.199	2.450	1.829	1.923	1.473
side-on η²- superoxo Cu(II)	2.130	2.153	2.153	1.910	1.806	1.339
end-on η¹- superoxo Cu(II)	2.166	2.103	2.067	1.858		1.468

All bond length in Å unit. Atom Numbering: N1 right , N2 centre and N3 left side nitrogen, O1 front and O2 back side oxygen, O--O peroxy oxygen

Figure 9. DFT stabilized structures of $\mu(\eta^2\text{-}\eta^2)$ peroxo dicopper(II), η^2- superoxo Cu(II), η^1- superoxo Cu(II) complexes.

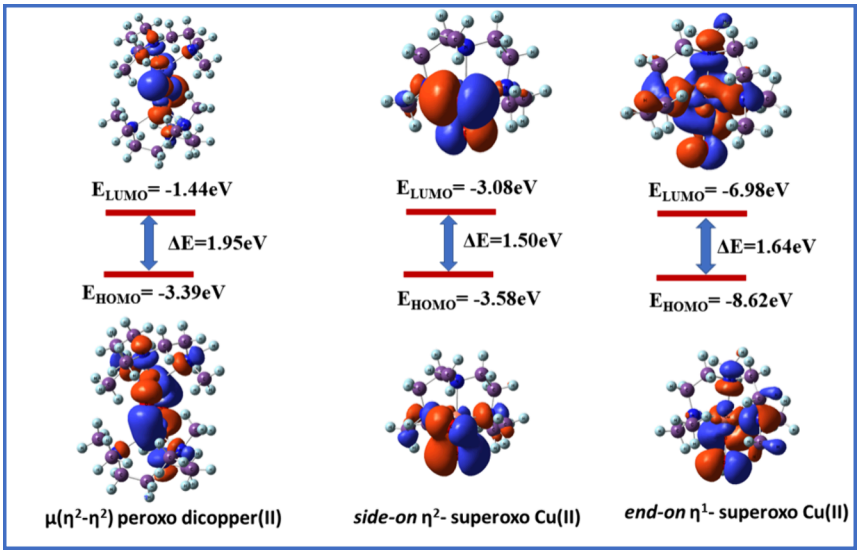

Figure 10. HOMO-LUMO energy levels of $\mu(\eta^2\text{-}\eta^2)$ peroxo dicopper(II), η^2- superoxo Cu(II), η^1- superoxo Cu(II) complexes.

(Scheme 2). Other reactive species like $[PMDETA]^{+\cdot}$ formed during irradiation could be combined with the bromine radical resulting in the formation of a radical cation ligand, ($PMDETA^{+\cdot}$ Br^-).

Scheme 2. Proposed Mechanism of Open-Air Photo ATRP of MMA

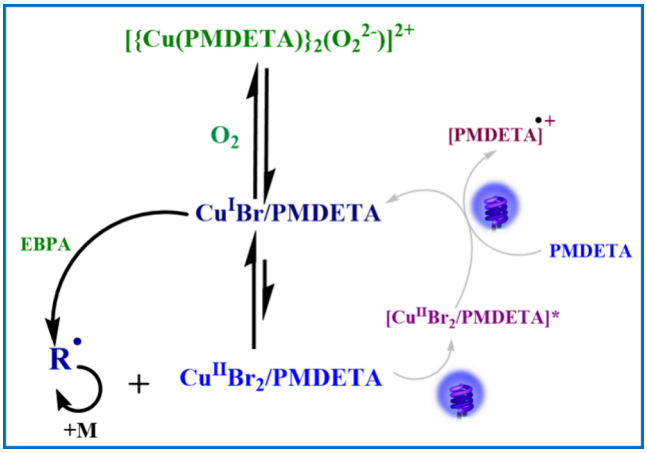

Like other ATRP systems, the amount of dead polymer chains formed due to the bimolecular termination in photo ATRP is negligible, if the rate of polymerization is considerably low. However, in the case of rapid polymerization, a significant amount of dead chain could be formed due to a higher concentration of radicals. In order to reduce the amount of dead chains, the polymerization time, initial monomer concentration $[M]_0$, targeted degree of polymerization (DP_T) and targeted monomer conversion (p) need to be carefully manipulated. Dead chain fraction (DCF) can be calculated by using eq 1.

$$\mathrm{DCF} = \frac{[T]}{[R-X]} = \frac{2\mathrm{DP}_T k_t [\ln(1-p)]^2}{[M]_0 k_p^2 t} \quad (1)$$

As shown in Table 4, the DCF for MMA at 200 DP_T was 38% whereas the DCF value was significantly low for 100 DP_T under same polymerization conditions. These results indicate that in order to achieve high chain end functionality, the rate of the polymerization could be decreased or required to quench the polymerization at lower conversions. Detailed investigation

https://doi.org/10.1021/acsomega.4c02773
ACS Omega 2024, 9, 44916−44930

Table 4. Dead Chain Fraction Values of Open-Air Photo ATRP of MMA Estimated Usingeq 1[a]

Entry	DP_T	α (%)	t (min)	DCF (%)
1	200	65	100	38
2	100	65	90	23

[a] k_p and k_t values were estimated from literature.[70,71] $[M]_o$ = 9.4M

on DCF is currently under progress in our laboratory. It should be noted that, though DCF value depends on $k_t/(k_p)$,[2] it can be decreased by varying the temperature and pressure of polymerization.[72,73]

Effect of PMDETA Concentration. The synergistic effect of ligand concentration in oxygen tolerant photo ATRP has already been exemplified in closed vessel systems, wherein the excess ligand significantly reduces the induction period by rapid self-degassing. Mechanistically, it has been proven that the photo reduction of amine regenerates the active form of catalyst (Cu(I)Br/L) in the presence of oxygen/air. To determine the effect of PMDETA concentration under open-air conditions, polymerizations were performed with different concentrations of PMDETA. For instance, when six equivalents of PMDETA relative to the initiator concentration was employed, an enhanced rate of polymerization was observed.

In the case of equimolar or one-tenth equivalents, the rate of polymerization significantly decreases. These results demonstrate the acceleration of photo reduction of the deactivator complex ($CuBr_2$/PMDETA) to generate the activator complex. Though a faster rate of polymerization was observed for a higher concentration of PMDETA, it became detrimental to the control over polymerization as evidenced by the kinetic profile (Figure 11a, b). GPC traces of kinetics of 1.0 and 6.0 equivalent concentration of PMDETA employed in the open-air ATRP are given in Figure S3 a,b.

The loss of control could be attributed to possible side reactions during polymerization. Importantly, we realized that 0.1 equivalents of PMDETA was sufficient for the controlled polymerization of MMA under open-air condition.

Effect of $CuBr_2$ Concentration. To evaluate the minimum concentration of $CuBr_2$ required for well controlled polymerization under open-air condition, $CuBr_2$ concentration levels were varied with different feed ratios ranging from 500 ppm (0.1 equiv), 50 ppm (0.01 equiv), and 5 ppm (0.001 equiv).

As evident from kinetic analysis (Figure 12a, b), no significant changes either on rate of polymerization or on control over molecular weight and dispersity was observed, when the concentration was reduced from 500 to 50 ppm. However, further reduction of $CuBr_2$ to 5 ppm, resulted in a significant loss of control as evidenced by the larger disparity between theoretical and experimental molecular weight and broader dispersity values ($Đ \sim 1.65$). GPC traces of kinetics of 0.01 and 0.001 equiv concentration of $CuBr_2$ employed in the open-air ATRP are given in Figure S4a,b. These results suggested that 100 ppm of $CuBr_2$ catalyst was sufficient to achieve reasonable control over polymerization under open-air condition.

Effect of Light Intensity. Mosnáček and co-workers demonstrated a linear relationship between the intensity of light and the rate of propagation, and they deliberately adjusted the light intensity in order to reduce the inhibition period from 4 to 2 h.[43] We have evaluated the rate of propagation with respect to the light intensity. As can be seen from kinetic analysis, a faster rate of polymerization with controlled molecular weight and narrow dispersity was obtained with an intensity of 4.2 mW cm^{-2}.

On reduction of intensity to 0.5 mW cm^{-2}, a slower rate of polymerization was observed (Figure 13a). However, the molecular weight increased linearly as the function of monomer conversion (Figure 13b). GPC traces of kinetics of light intensity (0.5 mW cm^{-2}) are given in Figure S5. It should be noted that the rate of polymerization was nearly 10 times slower under dark conditions (entry 7, Table 2). These results demonstrate that the irradiation of ATRP solution with a reasonable intensity significantly contributes for the faster activation−deactivation cycles to yield well-controlled polymerization under open-air condition. It should also be noted that, apart from the aforementioned effect of PMDETA, $CuBr_2$ and light intensity in photo ATRP of MMA, the presonication of ATRP solution is essential for a successful well-controlled polymerization. For instance, when polymerization was

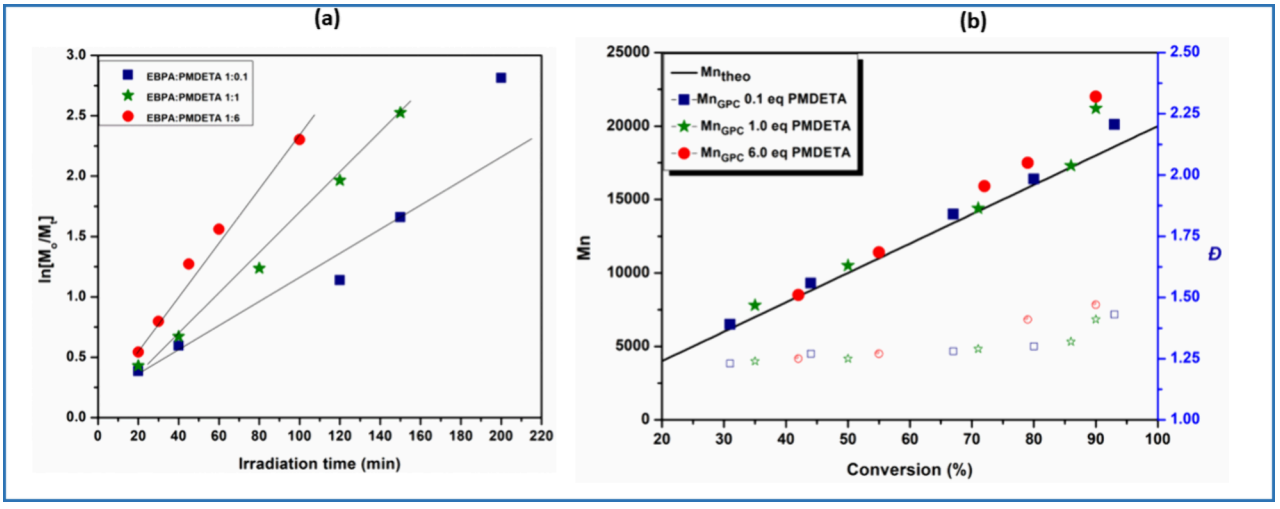

Figure 11. Effect of PMDETA concentration in open-air photo ATRP of methyl methacrylate. (a) Kinetic plot. (b) Evolution of molecular weight (solid points) and dispersity ($Đ$, hollow points) with monomer conversion. Experimental condition: MMA/EBPA/PMDETA/$CuBr_2$ = 200/1/0.1/X, X = 6 (red circle), X = 1 (green star), X = 0.1 (blue cube). 8 W domestic UV lamp λ = 365 nm, 4.2 mW cm^{-2}.

https://doi.org/10.1021/acsomega.4c02773
ACS Omega 2024, 9, 44916−44930

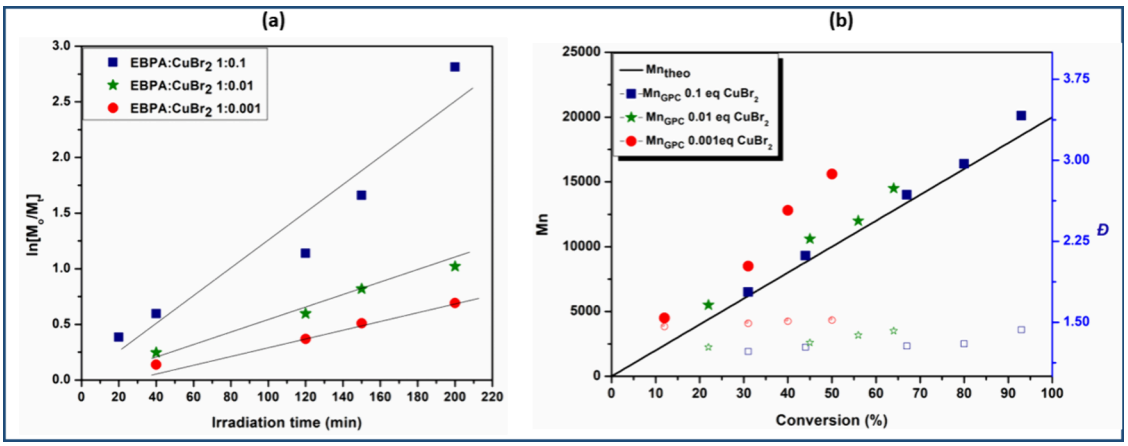

Figure 12. Effect of $CuBr_2$ concentration in open-air photo ATRP of Methyl methacrylate. (a) Kinetic plot. (b) Evolution of molecular weight (solid points) and dispersity ($Đ$, hollow points) with monomer conversion. Experimental conditions: MMA/EBPA/PMDETA/$CuBr_2$= 200/1/0.1/X; X = 0.1 (blue square); X = 0.01 (green star); X = 0.001 (red circle); 8W domestic UV lamp λ = 365 nm, 4.2 mW cm^{-2}.

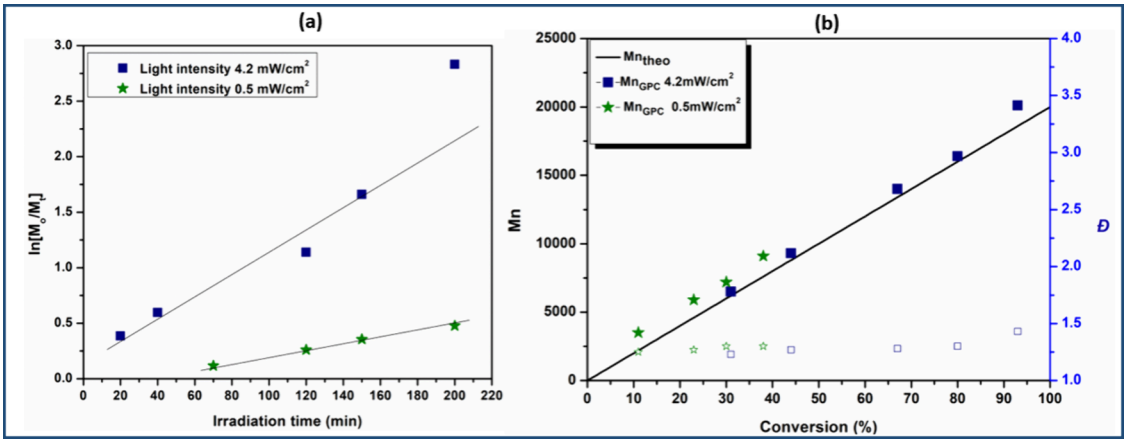

Figure 13. Effect of light intensity on-open-air photo ATRP of methyl methacrylate. (a) Kinetic plot. (b) Evolution of molecular weight (solid points) and dispersity ($Đ$, hollow points) with monomer conversion. Experimental conditions: MMA/EBPA/PMDETA/$CuBr_2$= 200/1/0.1/0.1; 8 W domestic UV lamp λ = 365 nm 4.2 mW cm^{-2} (blue square), 0.5 mW cm^{-2} (green star).

conducted without prior sonication, though reasonable correlation between experimental molecular weight and theoretical value was achieved, a major drift in the dispersity was invariably observed (entry 8, Table 2). Therefore, an appropriate irradiation source, its orientation with respect to position of reaction vessel and prior sonication of the reaction mixture are considered to be contributing factors for successful open-air photo ATRP of MMA.

Effect of Intermittent Irradiation (On−Off Cycle). In photo ATRP, it was possible to discontinue the polymerization for some interval of time by placing the reaction vessel into the dark confinement. Upon reexposure to the irradiation source, polymerization can be continued with an almost similar rate of propagation. We examined the temporal control in open-air polymerization by intermittent ON/OFF cycles of the light.

As can be seen from Figure 14, in all cycles, the rate of propagation was substantially reduced in the dark and accelerated upon irradiation to reach higher conversion. This temporal control behavior could be seen as direct evidence for the involvement of light in regeneration of the active form of the catalyst. These results suggest that light accelerates the rate of polymerization, enabling faster activation and deactivation cycles in the presence of $CuBr_2$/PMDETA coupled with atmospheric oxygen. It should be noted that the rate of

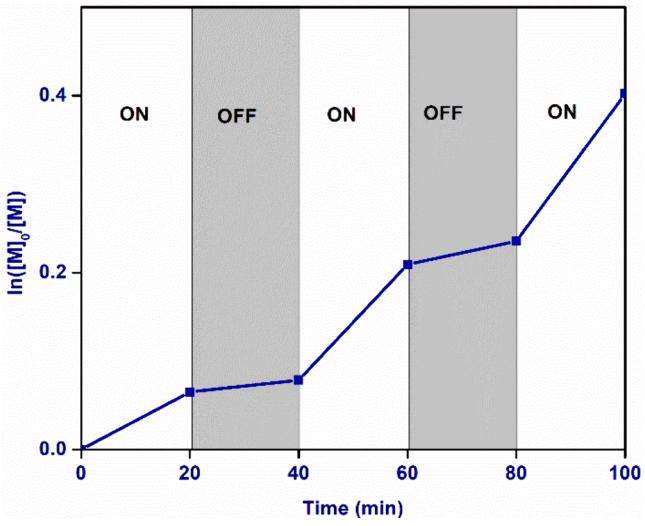

Figure 14. Effect of intermittent lights (ON/OFF cycles) in open-air ATRP. Experimental conditions: MMA/EBPA/PMDETA/$CuBr_2$= 200/1/0.1/0.1; light ON (white area) and light OFF (shaded area); 8 W domestic UV lamp λ = 365 nm; 4.2 mW cm^{-2}.

https://doi.org/10.1021/acsomega.4c02773
ACS Omega 2024, 9, 44916−44930

polymerization was not completely halted during the dark period. This could be explained by low activity of CuBr(I)/PMDETA, which led to slower dormancy in the dark, i.e., the presence of residual CuBr(I)/PMDETA complex in the dark responsible for chain propagation.

Monomer Scope. The scope of open-air photo ATRP was successfully extended to other monomers including methyl acrylate (MA), benzyl methacrylate (BzMA) and glycidyl methacrylate (GMA) (Table 5). Kinetic investigation of MA indicated a significant induction period (Figure S6a). However, after that induction period, the molecular weight increased linearly as a function of monomer conversion (Figure S6b). GPC traces of kinetic samples are given in Figure S6c. On the other hand, negligible induction period was observed for the polymerization of GMA (Figure S7a). The molecular weight increased linearly as a function of monomer conversion (Figure S7b). GPC traces of polymerization kinetics at subsequent intervals are given in Figure S7c. In the case of open-air photo ATRP of BzMA, a faster rate of polymerization with negligible induction period was observed (Figure S8a). The molecular weight increased linearly as the function of monomer conversion (Figure S8b). GPC traces of kinetic samples are given in Figure S8c. In the case of styrene (St), a kinetic investigation by ^{1}HNMR under open-air condition indicated only a negligible conversion even after 48 h of irradiation (Figure S9) under open-air condition. However, a well-controlled polymerization of styrene under non degassed closed conditions was observed. Kinetic study results are given in Figure S10a,b.c.

Table 5. Open-Air Photo ATRP of Different Monomers[a]

Monomer	[MMA]/[$CuBr_2$]/[L]/[EBiB]	Time (min)	α (%)	Mn_{theo}	Mn_{GPC}	$Đ$
MA	200/0.1/0.1/1	360	77	13200	19500	1.45
BzMA	200/0.1/0.1/1	60	72	25400	36800	1.50
GMA	200/0.1/0.1/1	60	75	21300	31900	1.49
[b]**St**	50/0.1/0.1/1	48h	66	3400	3500	1.19

[a]Order of addition and polymerizations were performed as per same procedure given in the Figure 1a. For the polymerization of MA, Me_6Tren was used as the ligand. For other monomers PMDETA was used as the ligand. [b]Nondegassed closed condition.

Chain Extension Analysis. In order to determine the chain end functionality, chain extension was performed using the macroinitiator PMMA-Br (Mn = 4700, $Đ$ = 1.29) under open-air conditions. A clear shift of the GPC peak (Figure 15a) from lower molecular weight to higher molecular weight (Mn = 19200 and $Đ$ = 1.52) demonstrates the living nature of the polymer chain end. The synthesis of a poly (methyl methacrylate)-*b*-(benzyl methacrylate) diblock copolymer (Figure 15b) under open-air condition indicates the high chain end functionality. Additionally, the chain end functionality of the polymer was confirmed by MALDI-ToF MS

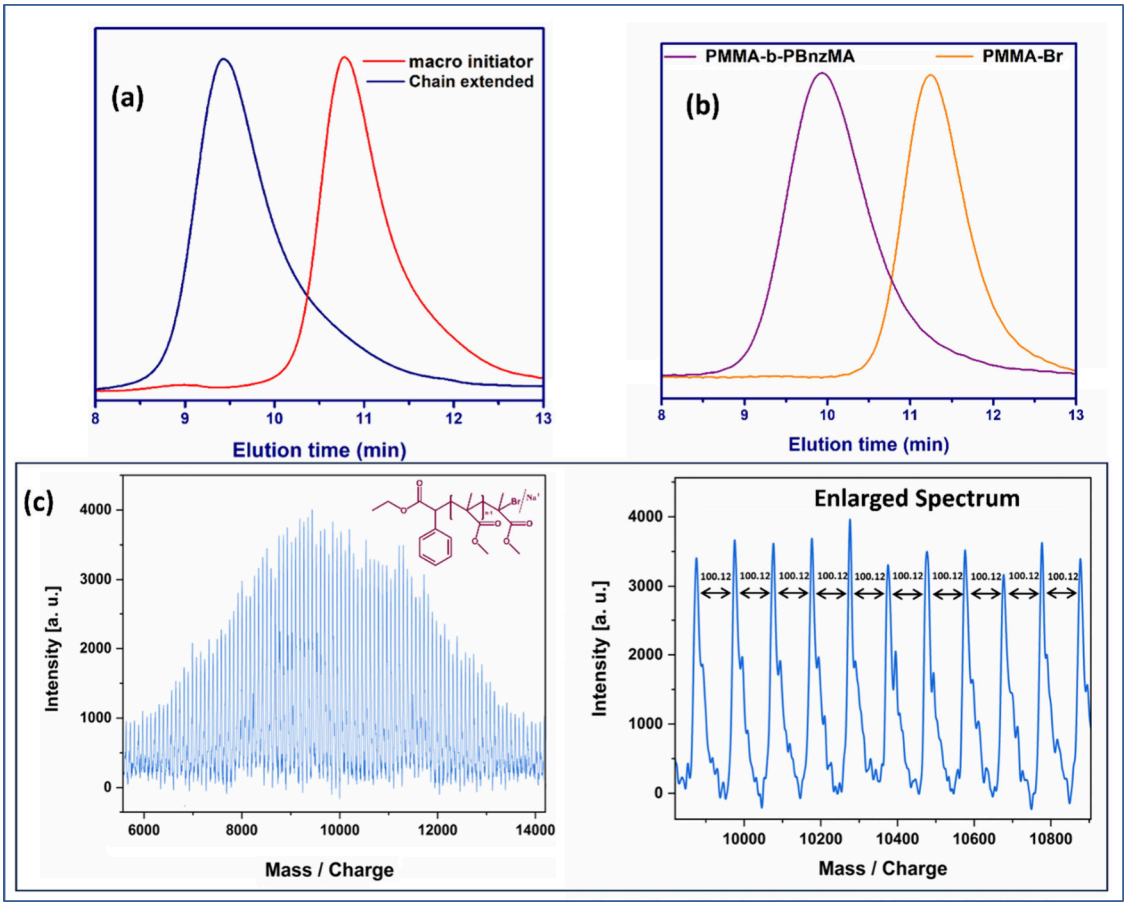

Figure 15. GPC traces of (a) PMMA macroinitiator (PMMA-Br, red) followed by homo chain extension (blue) and (b) hetero chain extension using BzMA (PMMA-Br, red and PMMA-b-PBzMA diblock copolymer, blue); (c) MALDI -ToF analysis of PMMA-Br prepared under open-air condition.

https://doi.org/10.1021/acsomega.4c02773
ACS Omega 2024, 9, 44916−44930

analysis. As shown in the enlarged spectrum (Figure 15c), the main series of peaks with the interval of 100.121 corresponds to PMMA with one bromine atom at the ω-end. All of these results confirm the chain end functionality.

CONCLUSIONS

In summary, we have reported a simple polymerization methodology for the facile synthesis of PMMA under mild condition. Rapid polymerization with moderate control was observed even under nondegassed open-air condition. The controlled nature of polymerization is most likely attributed to the regeneration of active form of catalyst by the reversible oxygen binding mechanism in $[\{Cu\ (PMDETA)\}_2(O_2^{2-})]^{2+}$. The scope of the presented methodology was also extended to other monomers including MA, GMA and BzMA. Though styrene was not polymerized under open-air condition, a well-controlled polymerization was observed under nondegassed closed vessel condition. The chain extension analysis such as synthesis of poly (methyl methacrylate)-*b*-(benzyl methacrylate) diblock copolymer and MALDI-ToF MS analysis supported the livingness of polymer chain prepared under open-air condition. More detailed mechanistic investigation of the present work would provide a better understanding to synthesize well-controlled polymers in the presence of oxygen.

ASSOCIATED CONTENT

Supporting Information

The Supporting Information is available free of charge at https://pubs.acs.org/doi/10.1021/acsomega.4c02773.

Kinetic plots and GPC traces of polymerizations under varied condition; ^{1}H NMR spectroscopy study of photo ATRP of styrene under open-air condition (PDF)

AUTHOR INFORMATION

Corresponding Author

Kannapiran Rajendrakumar − *Centre for Advanced Materials and Innovative Technologies (CAMIT), Vellore Institute of Technology, Chennai 600127, India;* orcid.org/0000-0001-8697-2705; Email: rajendrakumar.k@vit.ac.in

Author

Arumugam Ramu − *Department of chemistry, School of Advanced Sciences, Vellore Institute of Technology, Chennai 600127, India*

Complete contact information is available at: https://pubs.acs.org/10.1021/acsomega.4c02773

Notes

The authors declare no competing financial interest.

ACKNOWLEDGMENTS

The authors thank Vellore institute of technology Chennai for providing "VIT RGEMS SEED GRANT" for carrying out this research work. We also thank Prof. R. Kothandaraman, IIT Madras, India for the electrochemical measurements.

REFERENCES

(1) Lorandi, F.; Fantin, M.; Matyjaszewski, K. Atom Transfer Radical Polymerization: A Mechanistic Perspective. *J. Am. Chem. Soc.* **2022**, *144* (34), 15413−15430.

(2) Perrier, S. 50th Anniversary Perspective: RAFT Polymerization A User Guide. *Macromolecules* **2017**, *50* (19), 7433−7447.

(3) Gomollon-Bel, F. Ten Chemical Innovations That Will Change Our World: IUPAC identifies emerging technologies in Chemistry with potential to make our planet more sustainable. *Chemistry International* **2019**, *41* (2), 12−17.

(4) Matyjaszewski, K. Advanced materials by atom transfer radical polymerization. *Adv. Mater.* **2018**, *30* (23), 1706441.

(5) Dworakowska, S.; Lorandi, F.; Gorczynski, A.; Matyjaszewski, K. Toward green atom transfer radical polymerization: current status and future challenges. *Advanced Science* **2022**, *9* (19), 2106076.

(6) Matyjaszewski, K.; Tsarevsky, N. V. Macromolecular engineering by atom transfer radical polymerization. *J. Am. Chem. Soc.* **2014**, *136* (18), 6513−6533.

(7) Gao, H.; Matyjaszewski, K. Synthesis of star polymers by a combination of ATRP and the "click" coupling method. *Macromolecules* **2006**, *39* (15), 4960−4965.

(8) Pan, X.; Fantin, M.; Yuan, F.; Matyjaszewski, K. Externally controlled atom transfer radical polymerization. *Chem. Soc. Rev.* **2018**, *47* (14), 5457−5490.

(9) Dadashi-Silab, S.; Doran, S.; Yagci, Y. Photoinduced electron transfer reactions for macromolecular syntheses. *Chem. Rev.* **2016**, *116* (17), 10212−10275.

(10) Pan, X.; Tasdelen, M. A.; Laun, J.; Junkers, T.; Yagci, Y.; Matyjaszewski, K. Photomediated controlled radical polymerization. *Prog. Polym. Sci.* **2016**, *62*, 73−125.

(11) Dadashi-Silab, S.; Pan, X.; Matyjaszewski, K. Photoinduced iron-catalyzed atom transfer radical polymerization with ppm levels of iron catalyst under blue light irradiation. *Macromolecules* **2017**, *50* (20), 7967−7977.

(12) Tasdelen, M. A.; Uygun, M.; Yagci, Y. Studies on Photoinduced ATRP in the Presence of Photoinitiator. *Macromol. Chem. Phys.* **2011**, *212* (18), 2036−2042.

(13) Tasdelen, M. A.; Ciftci, M.; Yagci, Y. Visible light-induced atom transfer radical polymerization. *Macromol. Chem. Phys.* **2012**, *213* (13), 1391−1396.

(14) Li, B.; Yu, B.; Zhou, F. Spatial Control over Brush Growth through Sunlight-Induced Atom Transfer Radical Polymerization Using Dye-Sensitized TiO2 as a Photocatalyst. *Macromol. Rapid Commun.* **2014**, *35* (14), 1287−1292.

(15) Dadashi-Silab, S.; Tasdelen, M. A.; Kiskan, B.; Wang, X.; Antonietti, M.; Yagci, Y. Photochemically mediated atom transfer radical polymerization using polymeric semiconductor mesoporous graphitic carbon nitride. *Macromol. Chem. Phys.* **2014**, *215* (7), 675−681.

(16) Dadashi-Silab, S.; Atilla Tasdelen, M.; Mohamed Asiri, A.; Bahadar Khan, S.; Yagci, Y. Photoinduced atom transfer radical polymerization using semiconductor nanoparticles. *Macromol. Rapid Commun.* **2014**, *35* (4), 454−459.

(17) Ciftci, M.; Tasdelen, M. A.; Yagci, Y. Sunlight induced atom transfer radical polymerization by using dimanganese decacarbonyl. *Polym. Chem.* **2014**, *5* (2), 600−606.

(18) Fors, B. P.; Hawker, C. J. Control of a living radical polymerization of methacrylates by light. *Angew. Chem., Int. Ed.* **2012**, *51* (35), 8850−8853.

(19) Alfredo, N. V.; Jalapa, N. E.; Morales, S. L.; Ryabov, A. D.; Le Lagadec, R.; Alexandrova, L. Light-driven living/controlled radical polymerization of hydrophobic monomers catalyzed by ruthenium (II) metalacycles. *Macromolecules* **2012**, *45* (20), 8135−8146.

(20) Treat, N. J.; Sprafke, H.; Kramer, J. W.; Clark, P. G.; Barton, B. E.; Read de Alaniz, J.; Fors, B. P.; Hawker, C. J. Metal-free atom transfer radical polymerization. *J. Am. Chem. Soc.* **2014**, *136* (45), 16096−16101.

(21) Corbin, D. A.; Miyake, G. M. Photoinduced organocatalyzed atom transfer radical polymerization (O-ATRP): precision polymer synthesis using organic photoredox catalysis. *Chem. Rev.* **2022**, *122* (2), 1830−1874.

(22) Zaborniak, I.; Chmielarz, P.; Wolski, K. Riboflavin-induced metal-free ATRP of (meth) acrylates. *Eur. Polym. J.* **2020**, *140*, 110055.

(23) Zaborniak, I.; Chmielarz, P. Comestible curcumin: From kitchen to polymer chemistry as a photocatalyst in metal-free ATRP of (meth) acrylates. *Journal of Industrial and Engineering Chemistry* **2022**, *105*, 481−490.
(24) Xu, J.; Shanmugam, S.; Duong, H. T.; Boyer, C. Organo-photocatalysts for photoinduced electron transfer-reversible addition−fragmentation chain transfer (PET-RAFT) polymerization. *Polym. Chem.* **2015**, *6* (31), 5615−5624.
(25) Kutahya, C.; Aykac, F. S.; Yilmaz, G.; Yagci, Y. LED and visible light-induced metal free ATRP using reducible dyes in the presence of amines. *Polym. Chem.* **2016**, *7* (39), 6094−6098.
(26) Liu, X.; Zhang, L.; Cheng, Z.; Zhu, X. Metal-free photoinduced electron transfer−atom transfer radical polymerization (PET−ATRP) via a visible light organic photocatalyst. *Polym. Chem.* **2016**, *7* (3), 689−700.
(27) Razeghi, R.; Kazemi, F.; Nikfarjam, N.; Shariati, Y.; Kaboudin, B. Visible photo-induced catalyst-free polymerization via in situ prepared dibromide. *Eur. Polym. J.* **2021**, *144*, 110195.
(28) Bhanu, V. A.; Kishore, K. Role of oxygen in polymerization reactions. *Chem. Rev.* **1991**, *91* (2), 99−117.
(29) Shenoy, R.; Bowman, C. N. Mechanism and implementation of oxygen inhibition suppression in photopolymerizations by competitive photoactivation of a singlet oxygen sensitizer. *Macromolecules* **2010**, *43* (19), 7964−7970.
(30) Shriver, D. F.; Drezdzon, M. A. *The manipulation of air-sensitive compounds*; John Wiley & Sons, 1986.
(31) Zaborniak, I.; Chmielarz, P.Ł; Matyjaszewski, K. Synthesis of riboflavin-based macromolecules through low ppm ATRP in aqueous media. *Macromol. Chem. Phys.* **2020**, *221* (4), 1900496.
(32) Ramu, A.; Rajendrakumar, K. Natural catalyst mediated ARGET and SARA ATRP of N-isopropylacrylamide and methyl acrylate. *Polym. Chem.* **2020**, *11* (3), 687−694.
(33) Pearson, R. M.; Lim, C.-H.; McCarthy, B. G.; Musgrave, C. B.; Miyake, G. M. Organocatalyzed atom transfer radical polymerization using N-aryl phenoxazines as photoredox catalysts. *J. Am. Chem. Soc.* **2016**, *138* (35), 11399−11407.
(34) Yeow, J.; Chapman, R.; Gormley, A. J.; Boyer, C. Up in the air: oxygen tolerance in controlled/living radical polymerisation. *Chem. Soc. Rev.* **2018**, *47* (12), 4357−4387.
(35) Matyjaszewski, K.; Coca, S.; Gaynor, S. G.; Wei, M.; Woodworth, B. E. Controlled radical polymerization in the presence of oxygen. *Macromolecules* **1998**, *31* (17), 5967−5969.
(36) Min, K.; Jakubowski, W.; Matyjaszewski, K. AGET ATRP in the presence of air in miniemulsion and in bulk. *Macromol. Rapid Commun.* **2006**, *27* (8), 594−598.
(37) Zhang, L.; Cheng, Z.; Shi, S.; Li, Q.; Zhu, X. AGET ATRP of methyl methacrylate catalyzed by FeCl3/iminodiacetic acid in the presence of air. *Polymer* **2008**, *49* (13−14), 3054−3059.
(38) Jakubowski, W.; Min, K.; Matyjaszewski, K. Activators regenerated by electron transfer for atom transfer radical polymerization of styrene. *Macromolecules* **2006**, *39* (1), 39−45.
(39) Gnanou, Y.; Hizal, G. Effect of phenol and derivatives on atom transfer radical polymerization in the presence of air. *J. Polym. Sci., Part A: Polym. Chem.* **2004**, *42* (2), 351−359.
(40) Liarou, E.; Whitfield, R.; Anastasaki, A.; Engelis, N. G.; Jones, G. R.; Velonia, K.; Haddleton, D. M. Copper-mediated polymerization without external deoxygenation or oxygen scavengers. *Angew. Chem.* **2018**, *130* (29), 9136−9140.
(41) Liarou, E.; Han, Y.; Sanchez, A. M.; Walker, M.; Haddleton, D. M. Rapidly self-deoxygenating controlled radical polymerization in water via in situ disproportionation of Cu (I). *Chemical science* **2020**, *11* (20), 5257−5266.
(42) Matyjaszewski, K.; Fu, L. F.; Russell, A. R.; Enciso, A. A breathing ATRP: fully oxygen tolerant polymerization inspired by aerobic respiration of cells. *Angew. Chem. Int. Ed* **2018**, *57*, 933−936.
(43) Enciso, A. E.; Fu, L.; Lathwal, S.; Olszewski, M.; Wang, Z.; Das, S. R.; Russell, A. J.; Matyjaszewski, K. Biocatalytic "Oxygen-Fueled" Atom Transfer Radical Polymerization. *Angew. Chem., Int. Ed.* **2018**, *57* (49), 16157−16161.
(44) Mosnáček, J.; Eckstein-Andicsova, A.; Borska, K. Ligand effect and oxygen tolerance studies in photochemically induced copper mediated reversible deactivation radical polymerization of methyl methacrylate in dimethyl sulfoxide. *Polym. Chem.* **2015**, *6* (13), 2523−2530.
(45) Yang, Q.; Lalevee, J.; Poly, J. Development of a robust photocatalyzed ATRP mechanism exhibiting good tolerance to oxygen and inhibitors. *Macromolecules* **2016**, *49* (20), 7653−7666.
(46) Borska, K.; Moravcikova, D.; Mosnacek, J. Photochemically induced ATRP of (meth) acrylates in the presence of air: the effect of light intensity, ligand, and oxygen concentration. *Macromol. Rapid Commun.* **2017**, *38* (13), 1600639.
(47) Zain, G.; Bondarev, D.; Dohanosova, J.; Mosnacek, J. Oxygen-Tolerant Photochemically Induced Atom Transfer Radical Polymerization of the Renewable Monomer Tulipalin A. *ChemPhotoChem.* **2019**, *3* (11), 1138−1145.
(48) Szczepaniak, G.; Łagodzinska, M.; Dadashi-Silab, S.; Gorczynski, A.; Matyjaszewski, K. Fully oxygen-tolerant atom transfer radical polymerization triggered by sodium pyruvate. *Chemical science* **2020**, *11* (33), 8809−8816.
(49) Kapil, K.; Jazani, A. M.; Szczepaniak, G.; Murata, H.; Olszewski, M.; Matyjaszewski, K. Fully Oxygen-Tolerant Visible-Light-Induced ATRP of Acrylates in Water: Toward Synthesis of Protein-Polymer Hybrids. *Macromolecules* **2023**, *56* (5), 2017−2026.
(50) Ti, Q.; Fang, L.; Bai, L.; Luo, H.; Sun, R.; Ba, X.; Chen, W. Hybrid of Organophotoredox-and Cu-Mediated Pathways Enables Atom Transfer Radical Polymerization with Extremely Low Catalyst Loading. *Macromolecules* **2023**, *56* (11), 4181−4189.
(51) Hu, X.; Szczepaniak, G.; Lewandowska-Andralojc, A.; Jeong, J.; Li, B.; Murata, H.; Yin, R.; Jazani, A. M.; Das, S. R.; Matyjaszewski, K. Red-Light-Driven Atom Transfer Radical Polymerization for High-Throughput Polymer Synthesis in Open Air. *J. Am. Chem. Soc.* **2023**, *145* (44), 24315−24327.
(52) Shanmugam, S.; Xu, J.; Boyer, C. Exploiting metalloporphyrins for selective living radical polymerization tunable over visible wavelengths. *J. Am. Chem. Soc.* **2015**, *137* (28), 9174−9185.
(53) Zhang, T.; Yeow, J.; Boyer, C. A cocktail of vitamins for aqueous RAFT polymerization in an open-to-air microtiter plate. *Polym. Chem.* **2019**, *10* (34), 4643−4654.
(54) Rolland, M.; Whitfield, R.; Messmer, D.; Parkatzidis, K.; Truong, N. P.; Anastasaki, A. Effect of polymerization components on Oxygen-Tolerant Photo-ATRP. *ACS Macro Lett.* **2019**, *8* (12), 1546−1551.
(55) Wurtele, C.; Gaoutchenova, E.; Harms, K.; Holthausen, M. C.; Sundermeyer, J.; Schindler, S. Crystallographic characterization of a synthetic 1:1 end-on copper dioxygen adduct complex. *Angew. Chem., Int. Ed.* **2006**, *45* (23), 3867−3869.
(56) Park, G. Y.; Qayyum, M. F.; Woertink, J.; Hodgson, K. O.; Hedman, B.; Narducci Sarjeant, A. A.; Solomon, E. I.; Karlin, K. D. Geometric and electronic structure of [{Cu (MeAN)} 2 (μ-η2: η2 (O22−))] 2+ with an unusually long O−O bond: O−O bond weakening vs activation for reductive cleavage. *J. Am. Chem. Soc.* **2012**, *134* (20), 8513−8524.
(57) Parkatzidis, K.; Truong, N. P.; Whitfield, R.; Campi, C. E.; Grimm-Lebsanft, B.; Buchenau, S.; Rubhausen, M. A.; Harrisson, S.; Konkolewicz, D.; Schindler, S.; Anastasaki, A. Oxygen-Enhanced Atom Transfer Radical Polymerization through the Formation of a Copper Superoxido Complex. *J. Am. Chem. Soc.* **2023**, *145* (3), 1906−1915.
(58) Casa, S. D.; Parkatzidis, K.; Truong, N. P.; Anastasaki, A. Oxygen-enhanced superoxido copper-catalyzed ATRP accelerated by light. *J. Polym. Sci.* **2023**, *61* (23), 3087−3094.
(59) Campi, C. E.; Parkatzidis, K.; Anastasaki, A.; Schindler, S. Unusual Stability of an end-on Superoxido Copper (II) Complex under Ambient Conditions. *Chemistry−A European Journal* **2024**, *30*, e202401634.
(60) Elwell, C. E.; Gagnon, N. L.; Neisen, B. D.; Dhar, D.; Spaeth, A. D.; Yee, G. M.; Tolman, W. B. Copper−oxygen complexes revisited:

https://doi.org/10.1021/acsomega.4c02773
ACS Omega 2024, 9, 44916−44930

structures, spectroscopy, and reactivity. *Chem. Rev.* **2017**, *117* (3), 2059−2107.
(61) Hatcher, L. Q.; Kenneth, D. K. Ligand influences in copper-dioxygen complex-formation and substrate oxidations. *Adv. Inorg. Chem.* **2006**, *58*, 131−184.
(62) Gan, Z H; Yu, G Q; Tay, B K; Tan, C M; Zhao, Z W; Fu, Y Q Preparation and characterization of copper oxide thin films deposited by filtered cathodic vacuum arc. *Journal of physics d: applied physics* **2004**, *37* (1), 81.
(63) Liu, B.-H.; Huber, M.; van Spronsen, M. A.; Salmeron, M.; Bluhm, H. Ambient pressure X-ray photoelectron spectroscopy study of room-temperature oxygen adsorption on Cu (1 0 0) and Cu (1 1 1). *Appl. Surf. Sci.* **2022**, *583*, 152438.
(64) Henson, M. J.; Vance, M. A.; Zhang, C. X.; Liang, H.-C.; Karlin, K. D.; Solomon, E. I. Resonance Raman investigation of equatorial ligand donor effects on the Cu2O22+ core in end-on and side-on μ-peroxo-dicopper (II) and bis-μ-oxo-dicopper (III) complexes. *J. Am. Chem. Soc.* **2003**, *125* (17), 5186−5192.
(65) Qiu, J.; Matyjaszewski, K.; Thouin, L.; Amatore, C. Cyclic voltammetric studies of copper complexes catalyzing atom transfer radical polymerization. *Macromol. Chem. Phys.* **2000**, *201* (14), 1625−1631.
(66) Ribelli, T. G.; Fantin, M.; Daran, J.-C.; Augustine, K. F.; Poli, R.; Matyjaszewski, K. Synthesis and characterization of the most active copper ATRP catalyst based on tris [(4-dimethylaminopyridyl) methyl] amine. *J. Am. Chem. Soc.* **2018**, *140* (4), 1525−1534.
(67) Anastasaki, A.; Nikolaou, V.; Zhang, Q.; Burns, J.; Samanta, S. R.; Waldron, C.; Haddleton, A. J.; McHale, R.; Fox, D.; Percec, V.; Wilson, P.; Haddleton, D. M. Copper (II)/tertiary amine synergy in photoinduced living radical polymerization: Accelerated synthesis of ω-functional and α, ω-heterofunctional poly (acrylates). *J. Am. Chem. Soc.* **2014**, *136* (3), 1141−1149.
(68) Frick, E.; Anastasaki, A.; Haddleton, D. M.; Barner-Kowollik, C. Enlightening the mechanism of copper mediated photoRDRP via high-resolution mass spectrometry. *J. Am. Chem. Soc.* **2015**, *137* (21), 6889−6896.
(69) Yan, W.; Dadashi-Silab, S.; Matyjaszewski, K.; Spencer, N. D.; Benetti, E. M. Surface-initiated photoinduced ATRP: Mechanism, oxygen tolerance, and temporal control during the synthesis of polymer brushes. *Macromolecules* **2020**, *53* (8), 2801−2810.
(70) Zhong, M.; Matyjaszewski, K. How fast can a CRP be conducted with preserved chain end functionality? *Macromolecules* **2011**, *44* (8), 2668−2677.
(71) Taylor, D. R.; van Berkel, K. Y.; Alghamdi, M. M.; Russell, G. T. Termination rate coefficients for radical homopolymerization of methyl methacrylate and styrene at low conversion. *Macromol. Chem. Phys.* **2010**, *211* (5), 563−579.
(72) Rzayev, J.; Penelle, J. HP-RAFT: a free-radical polymerization technique for obtaining living polymers of ultrahigh molecular weights. *Angew. Chem.* **2004**, *116* (13), 1723−1726.
(73) Kwiatkowski, P.; Jurczak, J.; Pietrasik, J.; Jakubowski, W.; Mueller, L.; Matyjaszewski, K. High molecular weight polymethacrylates by AGET ATRP under high pressure. *Macromolecules* **2008**, *41* (4), 1067−1069.

https://doi.org/10.1021/acsomega.4c02773
ACS Omega 2024, 9, 44916−44930